Contents

3. INJUN 5 Observations of Vehicle Potential Fluctuations at 2500 km

R. C. Sagalyn
Air Force Geophysics Laboratory
Hanscom AFB, Massachusetts

William J. Burke
Regis College Research Center
Weston, MA 92193

Abstract

The **AFCL** spherical electrostatic analyzers aboard the polar orbiting **Injun** 5 satellite were designed to measure the temperature and density of the plasma as well as the vehicle potential. Significant vehicle potential fluctuations have been observed at altitudes near **2500** km in the nighttime, topside ionosphere. At auroral latitudes, precipitating magnetospheric electrons frequently drive the satellite to such strongly negative potentials that the ambient electrons are shielded from our instruments. In such cases, simultaneous measurements by the **Iowa** State University **LEPEDEA** experiment can be uded **to** calculate the vehicle potential. Potentials of up **to -40** volts are observed during impulsive precipitation events. Within the plasma trough vehicle potentials vary between **-1.5** and **-4** volts, as compared with the **-0.5** to **-1** volt observed in the polar cap. The source of thts vehicle potential enhancement is ascribed to fluxes of photoelectrons that have escaped from the sunlit conjugate ionosphere,

I. INTRODUCTION

The potential of a satellite in the topside ionosphere varies in response to changing plasma parameters.[1-4] In this report, we discuss spacecraft charging mechanisms in the topside ionosphere utilizing data obtained by the two AFGL spherical electrostatic analyzers (SPA) aboard the polar-orbiting Injun 5 satellite.

The AFGL experiments on board Injun 5 are discussed elsewhere.[5] Briefly, Injun 5 was launched into polar orbit with an inclination of 81°, an apogee of 2543 km, and a perigee of 677 km. The two AFGL sensors are placed on 5 foot booms and, due to the satellite's magnetic alignment, are well outside the vehicle wake. A schematic of the probes given in Figure 1 shows that both the ion and electran SEA's consist of 1-inch diameter solid collectors surrounded by two wire mesh grids, The potentials of the collectors are set at -2000 and +100 volts. The outer grid of the ion SEA is groinded and the inner grid is held at t28 volts with respect to satellite ground, thus filtering ions with energies less than 28 volts. The electrofl sensor grids are electrically connected and are operated sequentially in two modes, each of 15.9 sec duration. In Mode 1, the grids are set at +6 volts. This positive resting bias is intended to counteract expected negative satellite potentials. In Mode 2, the grids are swept from -10 to +3 volts. Operating in these modes, we are normally able to measure the ambient electron temperature and density, the satellite potential, ana the omnidirectional flux of ions with energies greater than 28 eV.

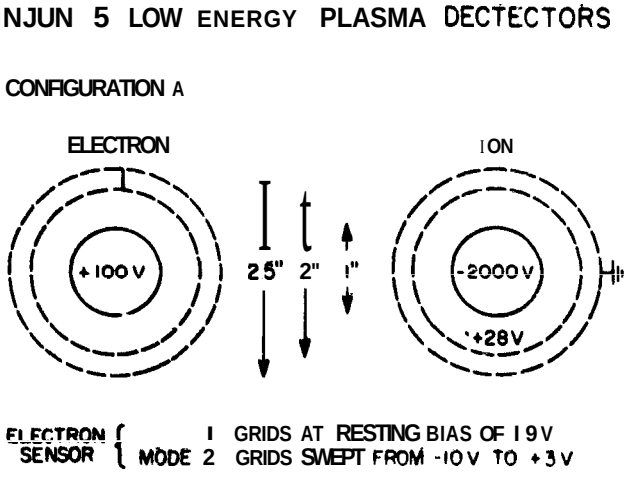

Figure 1. Schematic of the AFCL Electron and Ion Spherical Electrostatic Analyzers Aboard Injun 5

2. OBSERVATIONS

Results of vehicle potential measurements are discussed in terms of four typical cases. All data were tnkcn whtle the satellite was in darkness and near apogee over the northern hemisphere during December 1968. In the first (polar cap) and second (plasma trough) cases, the satellite potential was directly measured from Mode 2 current − voltage curves. The third and fourth cases were during soft and hard inverted-V precipitation events. Here the University of Iowa LEPEDEA measurements are used in Conjunction with those of the SEA to place bounds on the satellite potential.

Figure 2 gives a Mode 2 log I vs. V plot taken from the quiet time orbit No. 1463 while the satellite was in the polar cap region. For strongly retarding potentials, we note a steady background current which corresponds to a hyperthermal electron flux of 2 X Id7/cm~ sec. This flux is due to polar rain precipitation. 6 Near zero applied volts the curredt rises sharply, then approaches a saturation level id the electron acceleratioh region. We note that the applied voltage is relative to satellite ground. The applied voltage with respect to the plasma is found by algebraically adding the satellite potential.

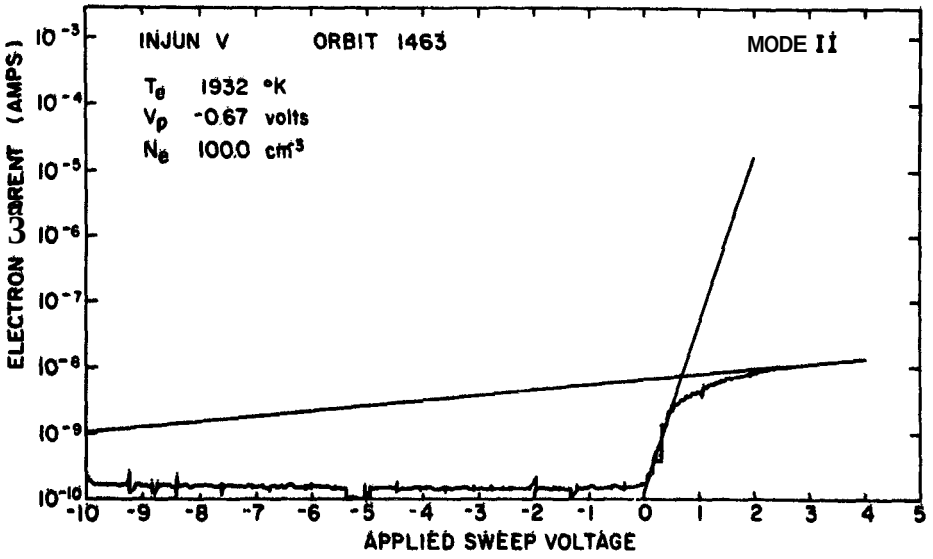

Figure 2. A Mode 2 Plot of log I versus V Taken while the Satellite was at −2500 km Over the Northern Winter Polar Cap

Electron temperatures T_e are calculated by assuming that the ambient plasma is Maxwelllan and applying the equations of Mott-Smith and Langmulr

$$T_e = \frac{q}{2.3k} \left[\frac{d \log_{10} I}{d V} \right]^{-1} \quad (1)$$

where q is the electroh charge and k the Boltzmann constant. A 50 point funning linear regression is performed on the data to determine the steepest slope in the retarding portidn of the curve and is used in Eq. (1). To calculate the vehicle potential, a linear regression is performed on the final 30 points of the Mode 2 log I vs V data. The potential at the intercept of the retarding and accelerating regression lines is the hegative of the satellite potential with respect to the plasma V_s

$$V_s = \text{intercept} \quad (2)$$

For the case presented in Figure 2, $n_e = 100\ cm^{-3}$, $T_e = 1932^{\circ}K$, arid $V_s = -0.67$ volt, where n_e is the ambient electron density.

The second example is taken from another quiet time orbit No. 1380 as the satellite passed through the midlatitude plasma trough (Figure 3). Using the methods described above, we calculate that $n_e = 100\ cm^{-3}$ and $T_e = 7600^{\circ}K$. Though the density is the same as in the first case, the temperature is a factor of four higher. Where lag I (V), in the extreme retarding portion of the sweep, was constant in the polar cap, here it rises linearly with increasing applied voltage. By calculating the solar zenith angle in the production region of the conjugate ionosphere, it can be shown that the hyperthermal electrons are photoelectrons from the sunlit southern hemisphere.[8] To the SEA, the conjugate photoelectrons appear as a nearly Maxwelliah population with a temperature of ~10 eV and a density of $\sim 4\ cm^{-3}$. Because the conjugate photoelectrons are efficient heaters of trough electrons,[9] they affect the satellite potential in two ways: (1) directly as a current away from the satellite, and (2) indirectly through enhahced thermal electron currents. Thus In the trough th&satellite potential was -1.65 volts as opposed to -0.67 volt in the polar cap.

It is to be expected that the most dramatic examples of tonospheric spacecraft charging are found in the nighttime auroral oval. We now consider the vehicle potential response to a low energy and a High energy inverted V prectpitation event.

The University of Iowa LEPEDEA[10] electron observations for the quiet orbit No, 1463 are given in Figure 4. Note that the more poleward inverted-V is marked by a sharp onset at 02:27:30 UT, a double peak in intensity, and maximum differential fluxes near a few hundred electron volts. SEA data for the same event are

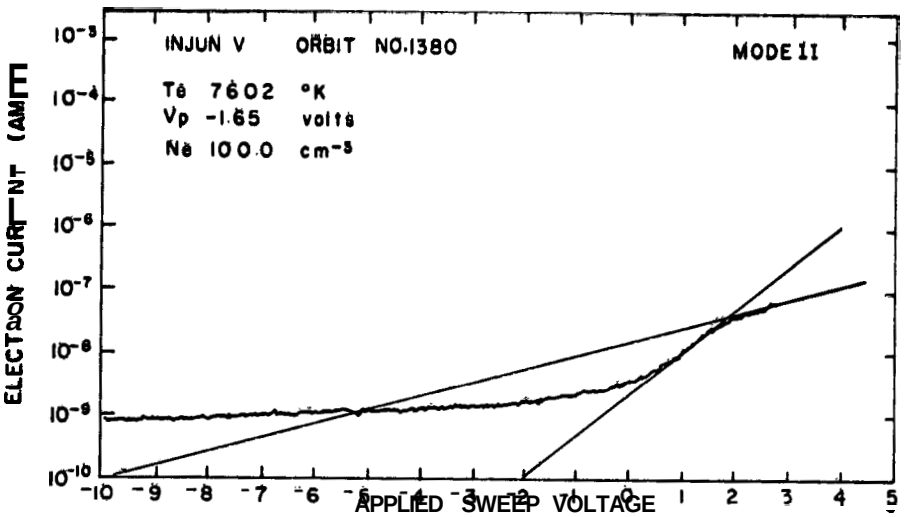

Figure 3. A Mode 2 Plot of log I versus V Taken while the Satellite was at ~2500 km Over the Winter Midlatitude Trough

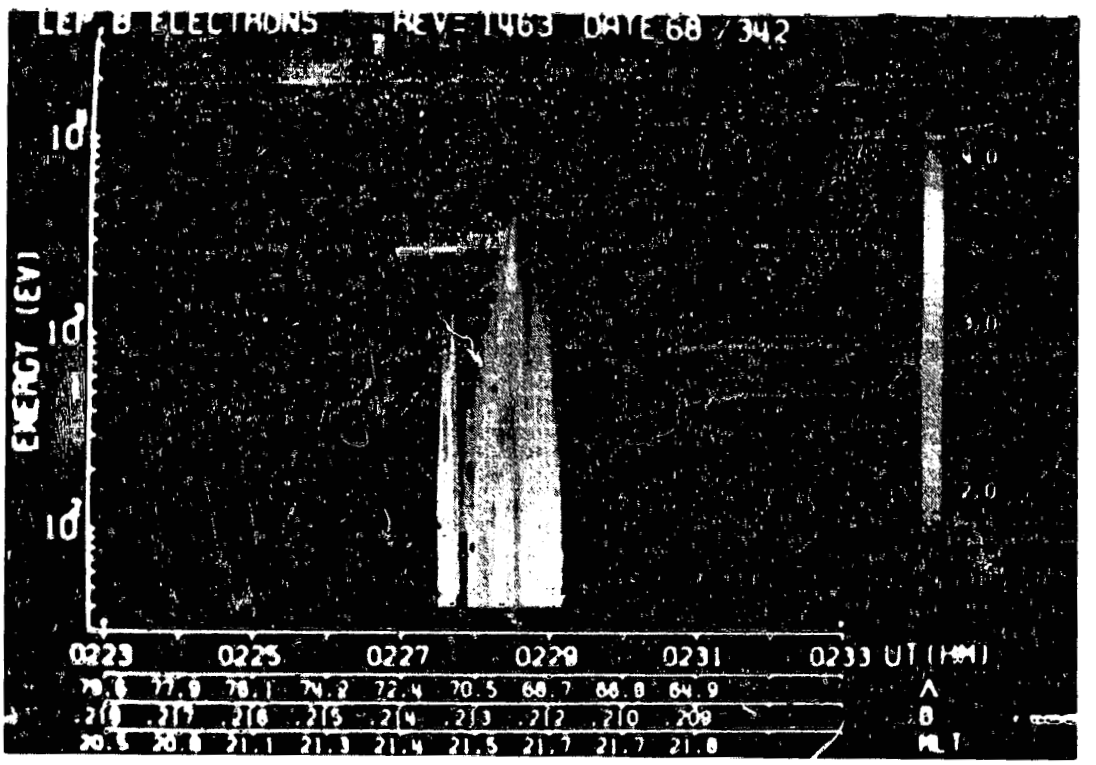

Figure 4. LEPEDEA Electron Spectragram From Injun 5 orbit No. 1463 (Prank and Ackerson)

shown in Figure 5, Omnidirectional fluxes of positive ions with E > 28 eV are given in the upper trace, and alternating Mode 1/Mode 2 electron fluxes are shown below. In the ion data, the inverted V_i at 02:27:30 UT appears as a flux enhancement with the same double peaked structure observed in the LEPEDEA electrons. The electron sensor was in Mode 1 with a grid resting bias of +6 volts at the start of this event. The total measured electron flux decreased as the precipitating flux increased and increased at the time of the valley between the two peaks. During the second half of the inverted V, event, the electron sensor switched to Mode 2. The anticorrelation between measured and precipitating fluxes durihg the Mode 1 portibn of the event indicates that the vehicle was being negatively charged. The flux measured in the extreme retarding portion of the subsequent Mode 2 sweep is a direct measurement of the omnidirectional flux of precipitating electrons.

The degree of charging during this low energy precipitation event can be estimated if we assume that the ambient plasma remained fairly constant through the

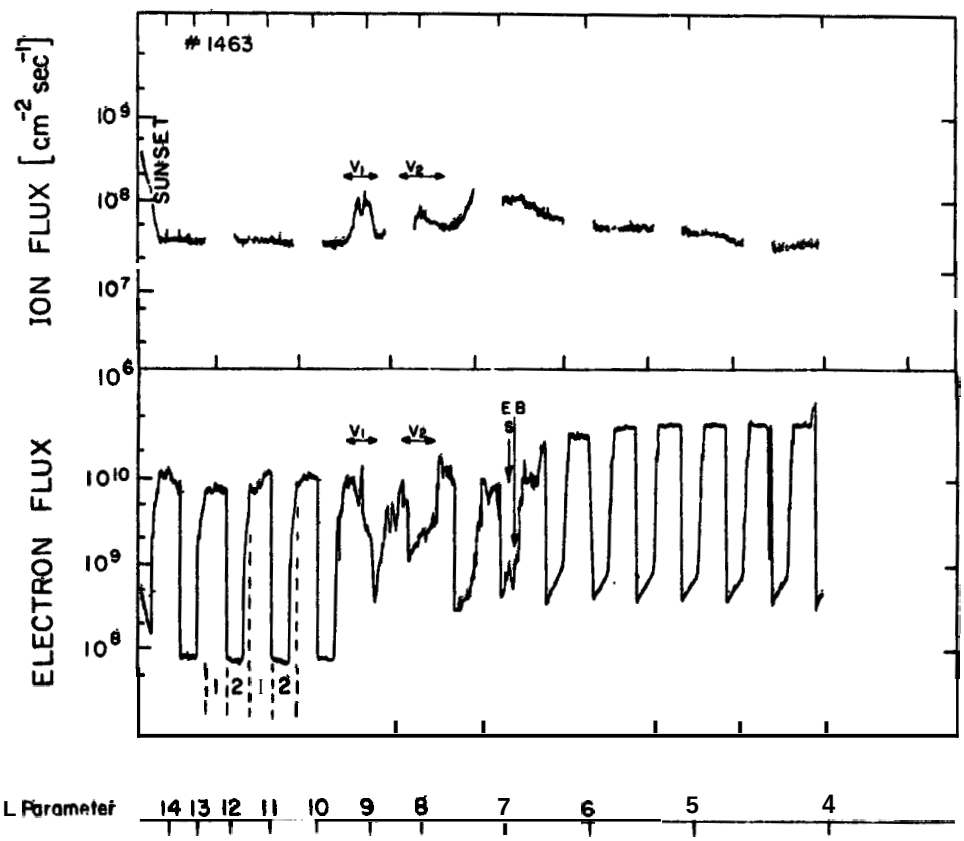

Figure 5. The Ion (Top Trace) and Electron (Bottom Trace) Flux Measurements During Orbit No. 1463

event. Since the resting bias of the grids was +6 volts, the flux measured during the Mode 1 portion was the sum of the thermal ahd hyperthermal flux that would be measured if the grids were biased at V - 6 + V_s. At 02:27:36 UT, the time of the first precipitation peak, the measured electron flux was 5. 5 × 16^9 cm^{-2} sec^{-1} (Figure 6). The measured flux at 02:27:42 UT, the ttme of the second precipitation

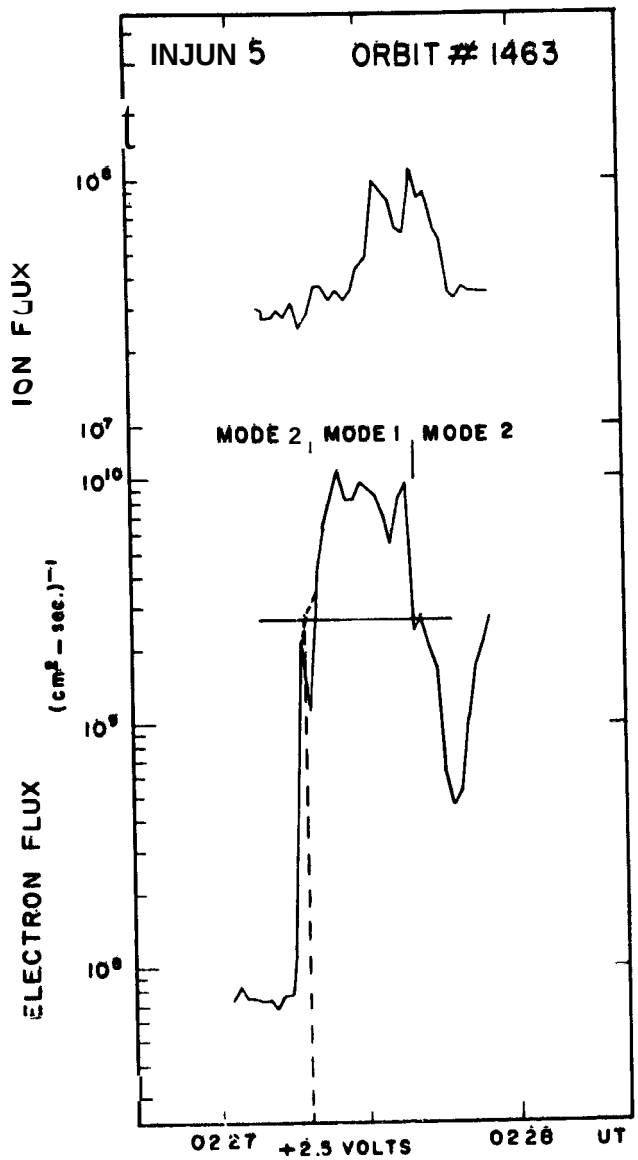

Figure 6. Same as Figure 5 for the Time Period 02:27:00 to 02:28:00 UT, Orbit No. 1463

peak, was 2.8×10^9 cm^{-2} sec^{-1}. Since the precipitating flux in the first and second peaks were about equal, the thermal electron flux contribution at 02:27:36 was $\sim 2.7 \times 10^9$ cm^{-2} sec^{-1}. We next compare this with the flux measured during the previous sweep. At 02:27:18 UT, a flux of 2.7×10^9 cm^{-2} sec^{-1} was measured with the sweep voltage was at +2.5 volts. This means that the satellite potential was approximately -3.5 vblts (2.5 - 6.0).

Satellite potential variatiohs typical of more intense precipitation events were observed duping orbit No. 1487. The LEPEDEA[11] electron observations for this orbit show adjacent inverted V's at 01:48:00 and 01:48:45 UT (Figure 7). Counting rates peak near 5 keV in the first, and at greater than 10 keV during the second inverted V event. The flux of electrons[11] with 50 ev $\leq$ E $\leq$ 15 kev and pitch angles of 0° and 90° are shown in Figure 8. The directional fluxes at these pitch angles were $\sim 10^9$ cm^{-2} sec^{-1} sr^{-1}, and generally within a factor of two of one another. The LEPEDEA[12] was unable to measure a field aligned proton fldx in the energy

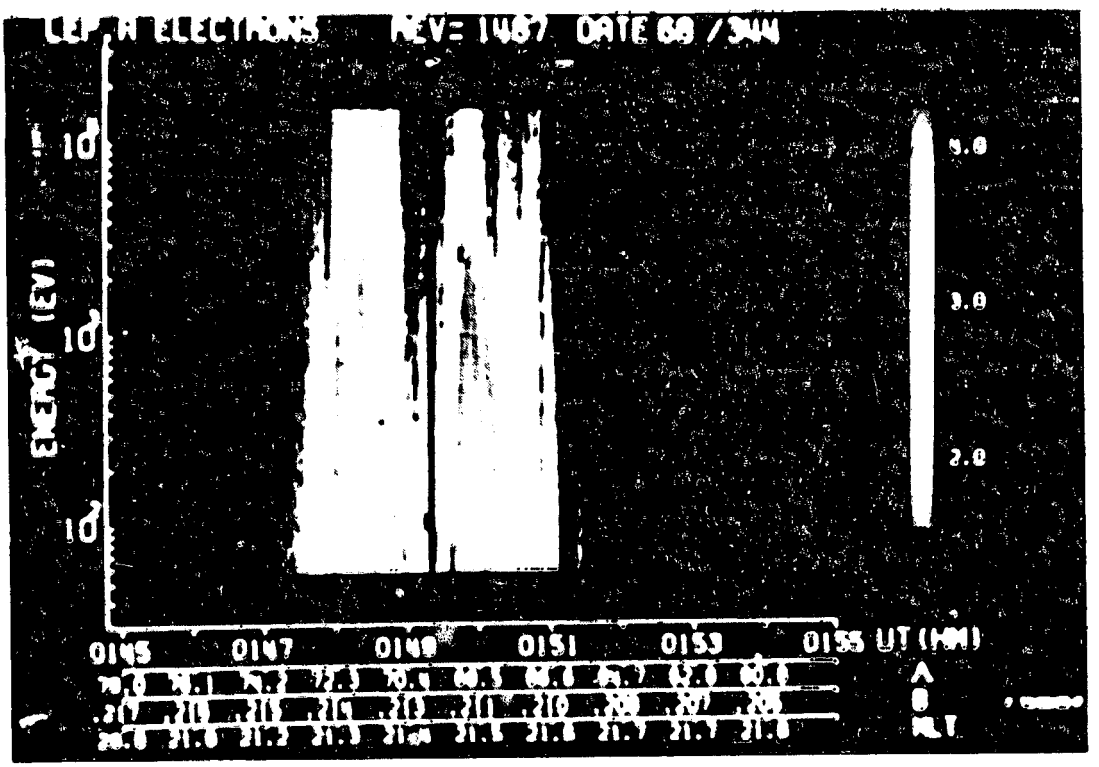

Figure 7. LEPEDEA Electron Spectragram From Injun 5 Orbit No. 1487 (Frank 1975).

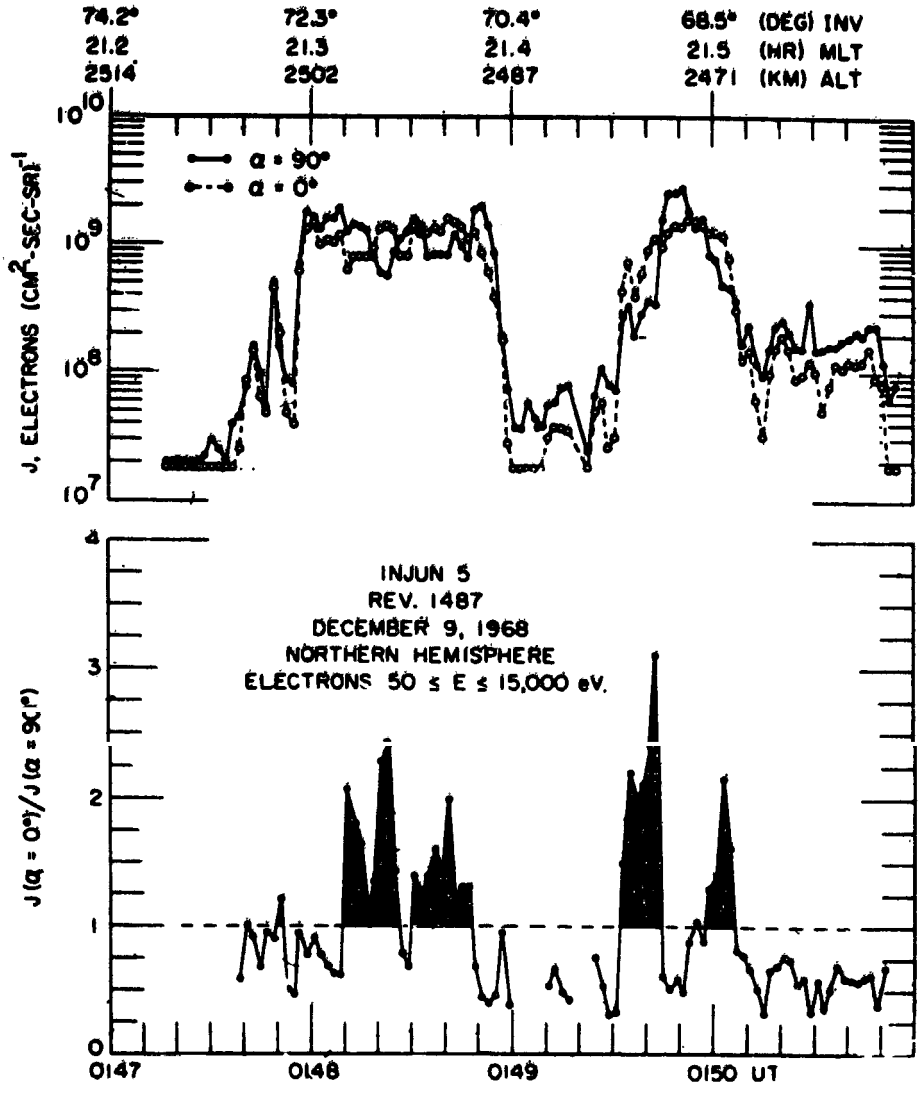

Figure 8. LEPEDEA Electron Fluxes at Pitch Angles of 0° and 90° in the Energy Range eV ≤ E ≤ keV During Inverted V Events of Orbit No. 1487 (Prank, 1975)

range 40 eV ≤ E ≤ 15 keV during these events (Figure 9). The SEA observations are given id Figure 10. It is impossible to distinguish between Mode 1 End Mode 2 fluxes during the second inverted V event. This is because ambient electron collection is completely suppressed by a satellite potential whose upper bound can be set at -6 volts (because of the +6 Mode 1 grid bias). During this period the Lon flux, thie upper trace of Figure 10, varied rapidly between 4×10^{6} and 8×10^{8} $cm^{-2} - sec^{-1}$. The lower value is a default level indicating that the current to the

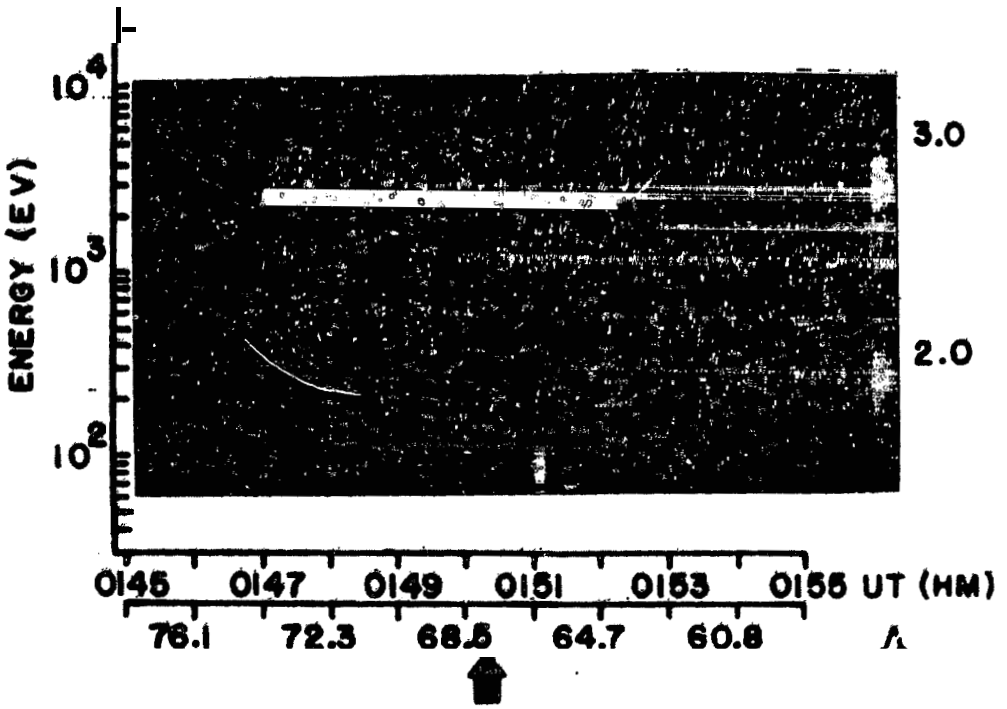

Figure 9. LEPEDEA **Proton** Spectragram From Injun 5 Orbit No. **1487** (Frank and Ackerson, **1972)**

ion sensor was negative, That is, the flux of electrons with E > 2 **keV,** the ion collector bias, exceeded the total ion flux.

The peak ion flux observed during the second inverted **V** of 8×10^8 cm^{-2} sec^{-1} could be due either to precipitating protons or to a combination **of** precipitating protons and ambient ions accelerated to the sensor by a negative satellite potential <-28 volts.

To test the first hypothesis, we first calculate the density **of** the parent electron population. If we assume that the precipitating flux is isotropic over the down **coming** hemisphere, then the total electron flux is

$$\phi_e = \frac{1}{2} n_e v_{th,e} \qquad (3)$$

where n_e and $v_{th,e}$ **are** the precipitating electron's density and mean thermal velocity in their magnetospheric source region. Their temperature is estimated from the LEPEDEA observations to be ~ **10** keV and their omnidirectional flux as

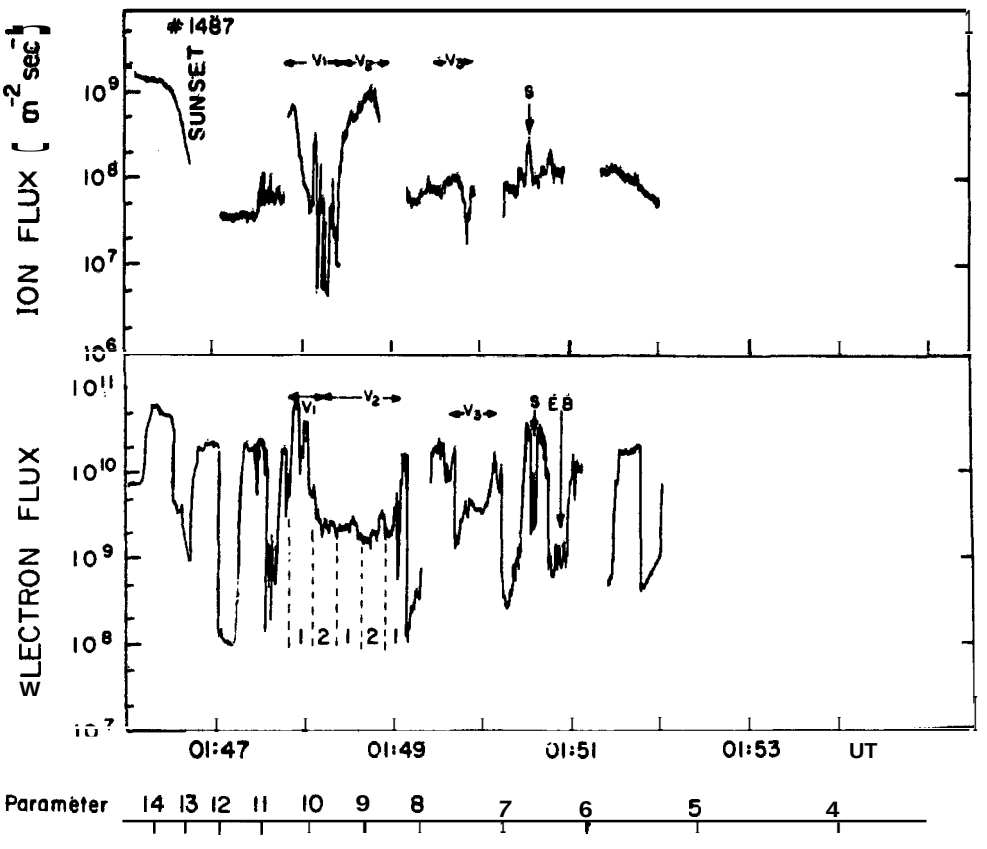

Figure 10. The Ion (Top Trace) and EleCtron (Bottom Trace) Fluxes Measured by the AFGL SEA During Injun 5 Orbit No. 1487

measured by the SEA is -2.5×10^9 cm^{-2} sec^{-1}. Substitution of these values into Eq. (3) gives a parent density of 0.83 cm^{-3}, a value typical of the plasma sheet. Assuming that the proton flux is isotropic and that $n_e \approx n_i$ in the source region, a flux of 8×10^8 cm^{-2} sec^{-1} implies a magnetospheric proton temperature of 480 keV. Thts is considerably higher than ahy measured proton temperature. Mozer and Bruston[13] have measured fluxes of precipitating protons with similar energies over an auroral form but with fluxes decreased by two orders of magnitude. We conclude that the ion flux cannot be due primarily to precipitating protons.

If we accept the second hypothesis that accelerated ambient ions are contributing to the measured flux, then an upper bound of -28 volts can be set on the vehicle potential. A lower bound of -40 volts can be set on the vehicle potential. There are 117 energy channels measured by LEPEDEA in the range 40 eV $\leq$ E $\leq$ 15 keV. It is highly unlikely that an ion flux of 8×10^8 could pass undetected.

Tho satellite potential adjusts itself so that the total current is zero. The precipitating electron flux is $\sim 2.5 \times 10^9$ cm^{-2} sec^{-1}. In the absence of an electron flux to the ion sensor, the measured ion flux would be equal to the electron flux. The electron flux to tho negatively biased ion sensor collector (-2 kV) is

$$\phi_{e,i} = 2.5 \times 10^9 \, e^{-qV/kT_e} \qquad (4)$$

where $\phi_{e,i}$ is the hyperthermal electron flux to the ion sensor, V 2000 volts, and $kT_e \approx 10$ keV. Thus $\phi_{e,i} \approx 2 \times 10^9$ cm^{-2} sec^{-1}. Thus the measured ion flux should be $\phi_{net} = 2.5 \times 10^9 - \phi_{e,i} = 5 \times 10^8$ cm^{-2} sec^{-1}. Given the uncertainty in the precipitating electron temperature in Eq. (4), this number compares favorably with the measured ion flux of 8×10^8 cm^{-2} sec^{-1}.

The vehicle charging hypothesis also helps to explain th&rapid variations in the ioh flux between high values and the default level near 01:48 UT of orbit No. 1487. Relatively small modulations of the vehicle potential above and below -28 volts allow the ion sensor grid to act as a gate determining whether ambient ions or energetic electrons reach the collector.

3. SUMMARY AND CONCLUSIONS

In this report, we have presented ioh and electron fluxes observed by the AFGL sensors aboard Injun 5. All data were taken while the satellite was in darkness. They can be used to establish typical values of spacecraft charging in the topside ionosphere. The vehicle potential was found to range from -0.67 volt in the cold tenuous plasma of the polar cap to $\sim$ -40 volts as the satellite passed through an intense auroral precipitation event. To a first approximation, the results are consistent with a simple flux balance calculation of the vehicle potential.

References

1. Beard, D. B., and Johnson, F. S. (1961) Ionospheric limitations on attainable satellite potential, J. Geophys. Res. 66:4113-4122.
2. Whipple, E.C. Jr. (1965) The equilibrium electric potential of a body in the upper atmosphere and in tnterplanetary space, NASA Rpt. X615-65-296, Goddard Space Flight Center, Greenbelt, MD.
3. Samir, U., and Willmore, A. P. (1966) The equilibrium potential of a spacecraft in the ionosphere, Planet. Sp. Sci. 14:1131-1137.

4. Kasha, M.A. (1969) The Ionosphere and Its Interaction with Satellites, Gordon and Breach, New York.

5. Burke, W.J., Dulong, F.D., and Sagalyn, R.C. (1976) Injun 9 observations of low energy plasma in the htgh latitude topside ionosphere, (submitted to J.Ceophys.Res.).

6. Winningham, J. D., and Heikkila, W.J. (1974) Polar cap auroral electron fluxes observed with ISIS I, J. Ceophys. Res. 79:949.

7. Mott-Smith, H. M., and Langmuir, I. (1926) The theory of collectors in gaseous discharges, Phys. Rev. 28:727.

8. Maier, E. J., and hao, B. C. N. (1968) Observations of the superthermal electron flux and electron temperatures at high latitudes, J. Geophys. Res. 75:7168.

9. Hanson, W. B. (1963) Electron temperatures in the upper atmosphere, Space Research 3:282.

10. Frank, L.A., and Ackerson, K. L. (1971) Observation of charged particle precipitation into the auroral zone, J. Ceophys. Res. 76:3612-3641.

11. Frank, L. A. (1975) Magnetospheric and auroral plasmas: a short survey of progress, Rev. Geophys. and Sp. Phys. 13:974.

12. Frank, L.A., and Ackerson, K. L. (1972) Local time survey of plasma at low altitudes over the auroral zone, J. Geophys. Res. 77:4116.

13. Mozer, F. S., and Bruston, P. (1968) Auroral zone proton-electron anti-correlations, protori angular distributions, and electric fields, J. Geophys. Res. 71:4461-4468.